Biogeosciences Discuss., 7, 3879–3910, 2010
www.biogeosciences-discuss.net/7/3879/2010/
doi:10.5194/bgd-7-3879-2010

Biogeosciences Discussions

Spatial and temporal variations in the sea surface pCO_2 and air-sea CO_2 flux in the equatorial Pacific: model sensitivity to gas exchange and biological formulations

X. J. Wang

Earth System Science Interdisciplinary Center, University of Maryland, College Park, MD 20740, USA

Received: 8 May 2010 – Accepted: 17 May 2010 – Published: 25 May 2010

Correspondence to: X. J. Wang (wwang@essic.umd.edu)

Published by Copernicus Publications on behalf of the European Geosciences Union.

Abstract

The equatorial Pacific Ocean is responsible for the interannual variability of the global ocean-atmosphere CO_2 fluxes. However, most ocean carbon models significantly underestimate the interannual variability of the regional ocean-atmosphere CO_2 fluxes. A basin-scale ocean circulation-biogeochemistry model is employed to investigate the uncertainties associated with the choice of gas exchange formulation, and to assess the implications of the choice of ecosystem model. Using four different, quadratic and cubic relationships of the gas transfer velocity with wind speed yields small differences in the integrated sea-to-air CO_2 flux (0.32 to 0.42 Pg C yr^{-1}), but large differences in the averaged ΔpCO_2 (44 to 73 µatm) for the area of 150° E–90° W, 10° N–10° S. While the choice of gas exchange formulation primarily influences the magnitudes, the choice of ecosystem model has a broader influence on the spatial and temporal variations in modeled carbon fields in the equatorial Pacific Ocean. Particularly, employing an ecosystem model without a dissolved organic pool overestimates the interannual variability in net community production, leading to under-estimated interannual variability of the basin-scale sea-to-air CO_2 flux.

1 Introduction

The equatorial Pacific Ocean plays a large role in the global carbon cycle. Thus, there have been extensive observations and regional modeling studies of oceanic partial pressure of CO_2 (pCO_2) and ocean-atmosphere CO_2 flux (Feely et al., 1995, 1999, 2002, 2004, 2006; Chai et al., 2002; Jiang and Chai, 2005, 2006; Wang et al., 2006b; Christian et al., 2008). On the one hand, a number of global carbon cycle modeling studies (Patra et al., 2005; Le Quéré et al., 2000; McKinley et al., 2004; Obata and Kitamura, 2003; Baker et al., 2006) indicate that the equatorial Pacific Ocean is responsible for the interannual variability of the global ocean-atmosphere CO_2 fluxes. On the other hand, there are still large discrepancies in estimates of the magnitude

BGD
7, 3879–3910, 2010

and the spatial and temporal variations among different approaches (e.g., observations, inverse models and ocean carbon forward models). Most ocean carbon models significantly underestimate the interannual variability of the regional ocean-atmosphere CO_2 fluxes (e.g., Christian et al., 2008; Wang et al., 2006b).

The rate of sea-air CO_2 flux is dependent on the gas exchange velocity (i.e., a function of wind speed) and the difference in pCO_2 between the atmosphere and sea surface. Algorithms relating the gas exchange velocity to wind speed have been developed based on field and/or laboratory studies (McGillis et al., 2001, 2004; Nightingale et al., 2000; Liss and Merlivat, 1986; Watson et al., 1991; Wanninkhof et al., 2004), and radiocarbon budgets (Wanninkhof et al., 1992, 1999). Current estimations of air-sea CO_2 fluxes are subject to errors due to uncertainties in several independent sources of variability, in particular the gas transfer velocity (Takahashi et al., 2002; Lee et al., 1998; Olsen et al., 2005; Naegler, 2009; Christian et al., 2008). Clearly, studies are still needed to assess the uncertainties associated with the use of gas exchange formulations at regional to global scales.

The pCO_2 variation in the surface water is controlled by physical, biological, and chemical processes. While the overall spatial and temporal variations of sea surface pCO_2 are dominated by physical processes in the tropical oceans, biological processes play an important role in modulating the variability of the carbon fluxes, and determining the strength of the tropical oceanic CO_2 source (Cosca et al., 2003; Rixen et al., 2005; Sabine et al., 2000; Wang et al., 2006b; Feely et al., 2006). It has been argued that the discrepancies, in particular the under-estimated interannual variability from models, may partly result from the overestimated export production (Obata and Kitamura, 2003). Interestingly, a global ocean modeling (Popova and Anderson, 2002) reports that modeled export production is not sensitive to the choice of ecosystem model whereas modeled sea surface pCO_2 is affected by inclusion of a dissolved organic pool. Recently, a regional modeling study (Christian et al., 2008) demonstrates that modeled carbon fields are sensitive to the parameterizations of biological processes. While these studies point out the importance of biological processes and

BGD
7, 3879–3910, 2010

parameterizations, little is known about how the biological formulations affect the spatial and temporal variations in the carbon fields.

In light of the importance of the equatorial Pacific and the fact that ocean carbon models underestimate the interannual variability of the basin-scale, ocean-atmosphere CO_2 fluxes, this study examines the potential influences of parameterizations of two main processes, i.e., gas transfer, and carbon uptake and regeneration pathways. The objectives of this study are to assess how these two parameterizations affect the spatial and temporal variations of the sea surface pCO_2 and ocean-atmosphere CO_2 fluxes, and to investigate if the choice of gas exchange formulation and/or ecosystem model can explain the underestimated interannual variability of the basin-scale outgassing in the equatorial Pacific.

2 Oceanographic characteristics

The equatorial Pacific consists of two distinct regions: the upwelling region in the Central and Eastern Pacific and the warm pool to the west (Picaut et al., 2001; Le Borgne et al., 2002). Under normal conditions, the upwelling region has shallower thermocline, and high nutrient concentrations in the surface waters. In contrast, the warm pool has a deeper thermocline and nutricline, with undetectable nutrient concentrations in the surface. As a result, the Central and Eastern equatorial Pacific often has mesotrophic conditions whereas the western warm pool experiences oligotrophic conditions. In general, primary production (PP) in the upwelling region (54 mmol C m^{-2} d^{-1}) is approximately twice of that in the warm pool (26 mmol C m^{-2} d^{-1}) (Le Borgne et al., 2002).

The surface water pCO_2 data from the past two decades indicate significant spatial-temporal variations (Feely et al., 1987, 1995, 2002, 2006; Takahashi et al., 1997, 2002, 2003, 2009). In addition, the size of the equatorial Pacific's carbon source shows strong interannual variability that is largely associated with the climate phenomenon, i.e., the El Niño/Southern Oscillation (ENSO). During the warm ENSO phase (i.e., El

BGD
7, 3879–3910, 2010

Niño years), the trade winds weaken, thus removing the driving force for upwelling and resulting in low concentrations of dissolved inorganic carbon (DIC) in the surface waters. These conditions lead to low sea surface pCO_2 and weak fluxes of CO_2 from the ocean to the atmosphere. Conversely, the trade winds are strong during non-El Niño years, producing strong upwelling that brings more DIC into the surface water. Hence the surface water pCO_2 is much higher and outgassing of CO_2 is stronger in the equatorial Pacific during the non-El Niño years than during the El Niño years.

3 Model descriptions

A fully coupled physical-biogeochemical model has been developed for the tropical Pacific. The ocean general circulation model (OGCM) is a reduced-gravity, primitive-equation, sigma-coordinate model that is coupled to an advective atmospheric mixed layer model (Murtugudde et al., 1996). The OGCM has 20 vertical layers with variable thicknesses. The upper-most layer, the mixed layer, is determined by surface turbulent kinetic energy generation, dynamic instability mixing, and convective mixing to remove static instabilities (Chen et al., 1994). The model is set up for the Pacific domain of 30° S–30° N with zonal resolution of 1°, and variable meridional resolutions of 0.3–0.6° between 15° S and 15° N (1/3° at latitudes <10°), increasing to 2° at the northern and southern boundaries. In the "sponge layer" (10° band) near the boundaries, temperature, salinity, nitrate and DIC are gradually relaxed back towards climatology.

The model is forced by solar radiation, cloudiness, surface wind stress, and precipitation. The air temperature and humidity are computed by the atmospheric mixed layer model. The solar radiation, precipitation, and cloudiness are climatological monthly means. The surface wind stresses are interannual, 6-day means from the National Centers for Environmental Prediction (NCEP) reanalysis (Kalnay et al., 1996). Initial conditions are taken from the outputs of a climatological run which has been spun up for 30 yr with initial conditions from the WOA98 atlas.

BGD
7, 3879–3910, 2010

A carbon chemistry model was implemented into the biogeochemical model (Wang et al., 2006b). The carbon model computes net community production (NCP) and air-sea CO_2 fluxes. The flux of CO_2 from the ocean to the atmosphere is calculated as:

$$FCO_2 = SK_0 \Delta pCO_2 \quad (1)$$

where S is the solubility of CO_2, which is a function of temperature and salinity (Weiss and Price, 1980). ΔpCO_2 is the difference in the pCO_2 between the sea surface and the atmosphere. K_0 is the gas transfer velocity, using the formulation of Wanninkhof (Wanninkhof, 1992):

$$K_0 = 0.31u^2 \left(\frac{Sc}{660}\right)^{-\frac{1}{2}} \quad (2)$$

where u is wind speed, and Sc is the Schmidt number calculated from temperature (T):

$$Sc = 2073.1 - 125.62T + 3.6276T^2 - 0.043219T^3 \quad (3)$$

4 Model experiments

There are two sets of model sensitivity studies. Both share one reference simulation, in which the Eq. (2) and an eleven-component ecosystem model (Fig. 1) are used. The biological components include large (L) and small (S) sizes of phytoplankton (P_S and P_L), zooplankton (Z_S and Z_L) and detritus (D_S and D_L), and dissolved organic nitrogen (DON). Model structure, equations and biological parameters were given by Wang et al. (2008).

4.1 Model sensitivity to gas exchange formulation

While there have been many studies suggesting various formulations for CO_2 air-sea exchange, commonly used formulations apply a relationship of the gas transfer velocity with wind speed, e.g., quadratic and cubic relationships. This sensitivity study

BGD
7, 3879–3910, 2010

consists of four simulations using the DON model: the reference run or W-92 (Wanninkhof, 1992), W-99 (Wanninkhof and McGillis, 1999), M-01 (McGillis et al., 2001) and M-04 (McGillis et al., 2004). The W-99, M-01 and M-04 formulations are given as, respectively:

$$K_0 = 0.0283u^3\left(\frac{Sc}{660}\right)^{-\frac{1}{2}}, \tag{4}$$

$$K_0 = \left(0.026u^3 + 3.3\right)\left(\frac{Sc}{660}\right)^{-\frac{1}{2}}, \tag{5}$$

$$K_0 = \left(0.014u^3 + 8.2\right)\left(\frac{Sc}{660}\right)^{-\frac{1}{2}}. \tag{6}$$

4.2 Model sensitivity to biological formulation

Biological processes affect the carbon cycle through NCP that is determined by carbon uptake (i.e., PP) and carbon regeneration (CR):

$$\mathrm{NCP} = \mathrm{PP} - \mathrm{CR} \tag{7}$$

Carbon regeneration formulation is largely dependent on ecosystem model structure. For the reference simulation, the CR is computed as:

$$\mathrm{CR} = 6.625\cdot(r_\mathrm{S}\mathrm{Z_S} + r_\mathrm{L}\mathrm{Z_L} + c_\mathrm{S}\mathrm{D_S} + c_\mathrm{L}\mathrm{D_L} + c_\mathrm{DON}\mathrm{DON}) \tag{8}$$

where r_S *and* r_L are the excretion coefficients for small and large zooplankton, respectively, and c_x, a rate for DON remineralization or detritus decomposition.

This study compares the reference simulation (i.e., the DON simulation) with another model simulation that employs a non-DON model (i.e., Wang et al., 2006a). The CR term in the non-DON model is computed as:

$$\mathrm{CR} = 6.625\cdot(r_\mathrm{S}\mathrm{Z_S} + r_\mathrm{L}\mathrm{Z_L} + c_\mathrm{S}\mathrm{D_S} + c_\mathrm{L}\mathrm{D_L}), \tag{9}$$

BGD
7, 3879–3910, 2010

Similar efforts have been made in model tuning and validation for both models, which result in some differences in the values of the common biological parameters (Table 1). As shown in Table 2, estimated PP rates from both models are in good agreements with the observations. For instance, the PP rate at 150° W, 0° in October 1994 is 95, 101 and 90–104 mmol C m^{-2} d^{-1} from the non-DON, DON model and the observation, respectively.

5 Model results

5.1 Sensitivity to gas exchange formulations

Figure 2 presents climatological means (1990–2007) of ΔpCO_2 and sea-to-air CO_2 flux using the DON model, showing considerable differences in the magnitude and spatial patterns among the four simulations that apply different relationships between the gas exchange coefficient and the wind speed. For the Wyrtki box, the W-99 simulation has the highest ΔpCO_2 (45–150 µatm) whereas the M-04 run produces the lowest values (30–120 µatm). There is a large degree of similarity in the magnitude and spatial pattern of ΔpCO_2 between the W-92 and the M-01 simulations, in which ΔpCO_2 ranges from <30 µatm in the western warm pool to 135 µatm in the cold tongue (Fig. 2a and c). Interestingly, the sea-to-air CO_2 flux reveals moderate differences between these two simulations, showing relatively larger spatial variability with higher values in the eastern equatorial Pacific in the W-92 run (~3.6 mol C m^{-2} yr^{-1}) than in the M-01 run (~3.2 mol C m^{-2} yr^{-1}). While the W-99 and the M-04 simulations have a similar range of sea-to-air CO_2 flux (i.e., 0.5–3 mol C m^{-2} yr^{-1}), there are pronounced differences in the spatial pattern between these two runs. The W-99 simulation produces the highest rates of outgassing between 6° S and 10° S whereas the M-04 run predicts the highest values in a relatively larger area (i.e., between 0° and 10° S). Despite the differences, all four simulations reproduce the observed meridional asymmetries of

BGD
7, 3879–3910, 2010

ΔpCO_2 and sea-to-air CO_2 flux in the equatorial Pacific (e.g., Feely et al., 2002, 2006; Takahashi et al., 2009).

The equatorial Pacific undergoes significant interannual changes in physical and biogeochemical processes that are largely associated with the ENSO events (McPhaden, 2003, 2006; Feely et al., 2002; Le Borgne et al., 2002; Wang et al., 2005, 2006b). Figure 3 shows the interannual variations of ΔpCO_2 and sea-to-air CO_2 flux from the model sensitivity study together with published ΔpCO_2 data. The W-92 and M-01 simulations reveal almost identical temporal variability, showing the lowest values (~30 µatm) during the strongest warm ENSO event in 1997/98. Previous observations showed that the ΔpCO_2 values dropped below 30 µatm in the entire equatorial Pacific during the period of November 1997 to May 1998 (Feely et al., 2002). Despite of the large differences in ΔpCO_2, all four simulations predict a rate of ~0.2 Pg yr^{-1} CO_2 released to the atmosphere during the 1997/98 El Niño. However, there are considerable differences in the integrated sea-to-air CO_2 flux among the four simulations during other periods. An early field based study suggests that for the area of 165° E–90° W, 5° N–10° S, the regional outgassing varies by a factor of 6 (i.e, 0.1 to 0.56 Pg C yr^{-1}) (Feely et al., 2004). Model simulations except the W-99 one show similar temporal variability (Fig. 3b).

5.2 Sensitivity to ecosystem model

A sensitivity study was carried out using the W-92 simulation. There are considerable differences in the magnitude and spatial patterns of ΔpCO_2 and sea-to-air CO_2 flux between the non-DON model and DON model (Fig. 4). The non-DON model predicts smaller spatial variability with a narrower range for both ΔpCO_2 (45–120 µatm) and sea-to-air CO_2 flux (1–3 mol C m^{-2} yr^{-1}) than the DON model (15–135 µatm and 0.5–3.5 mol C m^{-2} yr^{-1}). Large differences are found in the western warm pool where the non-DON model produces higher values for ΔpCO_2 and sea-to-air CO_2 flux relative to the DON model. Extensive observations have showed that ΔpCO_2 ranges from 0 to

BGD
7, 3879–3910, 2010

70 µatm, and sea-to-air CO_2 flux from 0 to 2 mol C m^{-2} yr^{-1} in this region (Feely et al., 2002, 2006; Takahashi et al., 1997, 2009). Thus, the DON model seems do a better job in simulating the spatial variability of ΔpCO_2 and sea-to-air CO_2 flux for the equatorial Pacific Ocean.

Apart from the difference in the magnitude, there are differences in the seasonal variations of ΔpCO_2 and sea-to-air CO_2 flux between the non-DON and DON models (Fig. 5). ΔpCO_2 seasonality shows considerable differences in the central-eastern equatorial Pacific whereas the seasonal sea-to-air CO_2 flux reveals moderate differences in the central equatorial Pacific. The non-DON model simulates a ΔpCO_2 peak in boreal fall in the central equatorial Pacific whereas the DON model produces a peak in spring in the eastern equatorial Pacific. A recent study suggests that the sea surface pCO_2 has a maximum in boreal spring-summer and a minimum in boreal fall-winter in the eastern equatorial Pacific (Jiang and Chai, 2006).

Figure 6 further shows the differences in seasonal anomalies (i.e, the seasonal climatology subtracted by the mean) of ΔpCO_2 and sea-to-air CO_2 flux. While both models produce similar seasonal anomalies in the eastern equatorial Pacific, the non-DON model simulates much weaker seasonal variability than the DON model. There are considerable differences in the western and central equatorial Pacific, particularly in the ΔpCO_2 anomaly near the dateline. For instance, ΔpCO_2 anomaly has a positive peak (>5 µatm) in boreal fall from the non-DON model, but in boreal spring from the DON model.

There are also pronounced differences in the interannual variability of ΔpCO_2 between the two simulations (Fig. 7). The non-DON model simulates much smaller temporal variability than the DON model. For example, ΔpCO_2 averaged for the Wyrtki box ranges from 70 to 125 µatm in the non-DON model, but from 45 to 120 µatm in the DON model. The largest differences in ΔpCO_2 are found during the warm ENSO events (e.g., in 1992–1993, 1997/98 and 2002). Similar to a previous modeling study (Popova and Anderson, 2002), the non-DON model predicts much higher values for ΔpCO_2 than the DON model on basin scale. As a result, total sea-to-air CO_2 flux is

BGD
7, 3879–3910, 2010

significantly higher in the non-DON model relative to the DON model (Fig. 7b), particularly during the warm events when there are large differences in ΔpCO_2 in the Wyrtki box.

6 Discussion

6.1 Implications of gas exchange formulations

There have been many studies addressing the uncertainties of regional to global ocean-atmosphere CO_2 fluxes in association with the choice of gas transfer formulation (Takahashi et al., 2002; Lee et al., 1998; Olsen et al., 2005; Naegler, 2009; Christian et al., 2008; Feely et al., 2004). A few studies indicate small differences in the integrated ocean-atmosphere CO_2 fluxes among the W-92, W-99, M-01 and M-04 (Olsen et al., 2005; Feely et al., 2004; Christian et al., 2008).

While this study shows that using the common gas transfer formulations of W-92, W-99, M-01 and M-04 results in small differences in the integrated sea-to-air CO_2 flux (i.e., from 0.32 to 0.44 Pg C yr^{-1}), this study also demonstrates large differences in the averaged ΔpCO_2 (i.e., from 44 µatm to 73 µatm) for the area of 150° E–90° W, 10° N–10° S during the period of 1990–2007 (Table 3). Most importantly, modeled sea-to-air CO_2 flux follows an order (M-04<W-92<M-01<W-99) that is exactly opposite to modeled ΔpCO_2 (W-99<M-01<W-92<M-04). Overall, the modeled ΔpCO_2 and sea-to-air CO_2 flux from both the W-92 simulation and M-01 simulation are in good agreements with observations (e.g., Feely et al., 2002, 2006; Takahashi et al., 2002, 2009) in terms of the magnitude and spatial variability.

A recent observation-based study using a formulation of $K_0=0.26u^2\left(\frac{Sc}{660}\right)^{-\frac{1}{2}}$ gives an estimate of 0.48 Pg C yr^{-1} outgassing for the year 2000 in the area of 140° E–90° W, 14° N–14° S (Takahashi et al., 2009). This modeling study (using $K_0=0.31u^2\left(\frac{Sc}{660}\right)^{-\frac{1}{2}}$)

BGD
7, 3879–3910, 2010

predicts a net sea-to-air CO_2 flux of 0.54 Pg C yr^{-1} (Table 5). It appears that model and data agree very well considering the difference in the formulation. However, the model simulates smaller outgassing for the year 1995 (0.49 Pg C yr^{-1}) than observation (0.52 Pg C yr^{-1}) that was based on an early dataset (Takahashi et al., 2002) but a new formulation (Takahashi et al., 2009). The modeled temporal variations in the carbon fields are in a good agreement with those in the equatorial Pacific by Feely et al. (2006). While there is strong evidence of increases in wind speed, ΔpCO_2 and outgassing in 2000 relative to 1995, there is possibility of high values in the carbon fields in 1995 than in 2000. As Table 5 illustrated, both ΔpCO_2 and outgassing vary significantly within 1995 and 2000 with large overlapping. Particularly, outgassing has a similar standard deviation (SD) to that during 1990–2007 (see Table 3). Clearly, model-data comparison needs to consider temporal variability at seasonal to interannual time scales.

6.2 Implications of biological formulations

Biogeochemical models are often validated by comparing modeled PP with observed values because PP has been one of the most widely measured biological parameters in the global ocean (e.g., Friedrichs et al., 2009; Wang et al., 2006b). However, sea surface DIC change is regulated by NCP rather than PP in terms of biogeochemical processes.

Figure 8 reveals a large degree of similarity in the integrated PP rate for the upper 50 m between the two models. For instance, both models produce much smaller PP rate in the warm waters (<20 mmol C m^{-2} d^{-1}) than in the cold tongue (~80 mmol C m^{-2} d^{-1}). However, CR rate is much higher in the non-DON model than in the DON model, leading to relatively lower NCP rate in the non-DON model. As illustrated in Table 4, the averaged CR rate for the Wyrtki box is 36 mmol C m^{-2} d^{-1} in the non-DON model, but 28 mmol C m^{-2} d^{-1} in the DON. Despite relatively small difference in the NCP rate (i.e., 11.9 vs. 12.6 mmol C m^{-2} d^{-1}), the non-DON model simulates

BGD
7, 3879–3910, 2010

much high values for ΔpCO_2 (94 µatm) and net sea-to-air CO_2 flux (0.25 Pg C yr^{-1}) than the DON model (80 µatm and 0.21 Pg C yr^{-1}).

For all the parameters, the relative differences (i.e., absolute difference divided by the mean) between the two models are smaller in the Wyrtki box (6–23%) than in the entire basin (9–48%). These results suggest that biological formulation has much larger impacts on modeled biogeochemical parameters in the non-upwelling area. Particularly, the most sensitive parameters are ΔpCO_2 and sea-to-air CO_2 flux that show significant increases (from 16–17% to 42–48%) in the relative difference.

Overall, the non-DON model predicts larger SD than the DON model for PP, NCP and CR. In contrast, ΔpCO_2 and net sea-to-air CO_2 flux show smaller SD in the non-DON model than in the DON model. The SD to mean ratio shows a modest decrease in NCP (from 33–38% to 21–27%) but a pronounced increase in both ΔpCO_2 (from 9–12% to 20–23%) and net sea-to-air CO_2 flux (from 16–24% to 32–33%) in the DON model relative to the non-DON model. These analyses demonstrate that the over-estimated NCP variability in the non-DON model may be largely responsible for the under-estimated interannual variations in the sea-to-air CO_2 flux (Wang et al., 2006b).

6.3 Other relevant issues and future work

The surface water pCO_2 is a function of DIC, sea surface temperature (SST), salinity (SSS) and alkalinity. While the surface DIC and SST may play a dominant role in the equatorial Pacific, the SSS and alkalinity are also important elements that are also subject to the seasonal-to-interannual variability associated with both ENSO precipitation and ocean circulation change.

The gas exchange coefficient, thus sea-to-air CO_2 flux, is strongly dependent on wind speed. Studies have demonstrated that the sea-air CO_2 exchange is sensitive to wind products (Olsen et al., 2005; Feely et al., 2004; Wanninkhof et al., 2004). However, apart from the effect on sea-air CO_2 exchange, wind strength directly drives the oceanic physical processes such as circulation and vertical mixing, thus determines

BGD
7, 3879–3910, 2010

SST, SSS and DIC. In addition, changes in winds have large impacts on biological activity. These physical and biological changes have complex influences on the carbon cycle in the equatorial Pacific. On the one hand, stronger winds bring cold, carbon-rich water into the surface, leading to a decrease in SST but an increase in DIC concentration. On the other hand, stronger winds also enhance biological activity (i.e., uptake of CO_2), compensating the increase of DIC concentration in the surface waters. Apparently, comprehensive analyses are needed to assess relative influence of wind products on both physical and biogeochemical processes.

Acknowledgements. This research is supported by grants from the National Aeronautics and Space Administration. The author wishes to acknowledge use of the Ferret program for analysis and graphics in this paper. Ferret is a product of NOAA's Pacific Marine Environmental Laboratory (Information is available at http://ferret.pmel.noaa.gov/Ferret/).

References

Aufdenkampe, A. K., McCarthy, J. J., Navarette, C., Rodier, M., Dunne, J., and Murray, J. W.: Biogeochemical controls on new production in the tropical Pacific, Deep-Sea Res. Pt. II, 49, 2619–2648, 2002.

Baker, D. F., Law, R. M., Gurney, K. R., Rayner, P., Peylin, P., Denning, A. S., Bousquet, P., Bruhwiler, L., Chen, Y. H., Ciais, P., Fung, I. Y., Heimann, M., John, J., Maki, T., Maksyutov, S., Masarie, K., Prather, M., Pak, B., Taguchi, S., and Zhu, Z.: TransCom 3 inversion intercomparison: impact of transport model errors on the interannual variability of regional CO_2 fluxes, 1988–2003, Global Biogeochem. Cy., 20, GB1002, doi:10.1029/2004GB002439, 2006.

Barber, R. T., Sanderson, M. P., Lindley, S. T., Chai, F., Newton, J., Trees, C. C., Foley, D. G., and Chavez, F. P.: Primary productivity and its regulation in the equatorial Pacific during and following the 1991–1992 El Nino, Deep-Sea Res. Pt. II, 43, 933–969, 1996.

Chai, F., Dugdale, R. C., Peng, T. H., Wilkerson, F. P., and Barber, R. T.: One-dimensional ecosystem model of the equatorial Pacific upwelling system. Part 1: Model development and silicon and nitrogen cycle, Deep-Sea Res. Pt. II, 49, 2713–2745, 2002.

BGD
7, 3879–3910, 2010

Chavez, F. P., Buck, K. R., Service, S. K., Newton, J., and Barber, R. T.: Phytoplankton variability in the Central and Eastern tropical Pacific, Deep-Sea Res. Pt. II, 43, 835–870, 1996.

Chen, D., Rothstein, L. M., and Busalacchi, A. J.: A hybrid vertical mixing scheme and its application to tropical ocean models, J. Phys. Oceanogr., 24, 2156–2179, 1994.

Christian, J. R., Feely, R. A., Ishii, M., Murtugudde, R., and Wang, X. J.: Testing an ocean carbon model with observed sea surface pCO_2 and dissolved inorganic carbon in the tropical Pacific Ocean, J. Geophys. Res.-Oceans, 113, C07047, doi:10.1029/2007jc004428, 2008.

Cosca, C. E., Feely, R. A., Boutin, J., Etcheto, J., McPhaden, M. J., Chavez, F. P., and Strutton, P. G.: Seasonal and interannual CO_2 fluxes for the central and eastern equatorial Pacific Ocean as determined from fCO_2-SST relationships, J. Geophys. Res., 108, doi:10.1029/2000JC000677, 2003.

Feely, R. A., Gammon, R. H., Taft, B. A., Pullen, P. E., Waterman, L. S., Conway, T. J., Gendron, J. F., and Wisegarver, D. P.: Distribution of chemical tracers in the Eastern equatorial Pacific during and after the 1982–83 El Niño/Southern Oscillation Event, J. Geophys. Res., 92, 6545–6558, 1987.

Feely, R. A., Wanninkhof, R., Cosca, C. E., Murphy, P. P., Lamb, M. F., and Steckley, M. D.: CO_2 distributions in the equatorial Pacific during the 1991–1992 ENSO event, Deep-Sea Res. Pt. II, 42, 365–386, 1995.

Feely, R. A., Wanninkhof, R., Takahashi, T., and Tans, P.: influence of El Nino on the equatorial Pacific contribution to atmospheric CO_2 accumulation, Nature, 398, 597–601, 1999.

Feely, R. A., Boutin, J., Cosca, C. E., Dandonneau, Y., Etcheto, J., Inoue, H. Y., Ishii, M., Quéré, C. L., Mackey, D. J., McPhaden, M., Metzl, N., Poisson, A., and Wanninkhof, R.: Seasonal and interannual variability of CO_2 in the equatorial Pacific, Deep-Sea Res. Pt. II, 49, 2443–2469, 2002.

Feely, R. A., Wanninkhof, R., McGillis, W., Carr, M. E., and Cosca, C. E.: Effects of wind speed and gas exchange parameterizations on the air-sea CO_2 fluxes in the equatorial Pacific Ocean, J. Geophys. Res., 109, C08S03, doi:10.1029/2003JC001896, 2004.

Feely, R. A., Takahashi, T., Wanninkhof, R., McPhaden, M. J., Cosca, C. E., Sutherland, S. C., and Carr, M. E.: Decadal variability of the air-sea CO_2 fluxes in the equatorial Pacific Ocean, J. Geophys. Res., 111, C08S90, doi:10.1029/2005JC003129, 2006.

Friedrichs, M. A. M., Carr, M.-E., Barber, R. T., Scardi, M., Antoine, D., Armstrong, R. A., Asanuma, I., Behrenfeld, M. J., Buitenhuis, E. T., Chai, F., Christian, J. R., Ciotti, A. M., Doney, S. C., Dowell, M., Dunne, J., Gentili, B., Gregg, W., Hoepffner, N., Ishizaka, J.,

Kameda, T., Lima, I., Marra, J., Mélin, F., Moore, J. K., Morel, A., O'Malley, R. T., O'Reilly, J., Saba, V. S., Schmeltz, M., Smyth, T. J., Tjiputra, J., Waters, K., Westberry, T. K., and Winguth, A.: Assessing the uncertainties of model estimates of primary productivity in the Tropical Pacific Ocean, J. Mar. Syst., 76, 113–133, 2009.

Jiang, M. S. and Chai, F.: Physical and biological controls on the latitudinal asymmetry of surface nutrients and pCO_2 in the Central and Eastern equatorial Pacific, J. Geophys. Res.-Oceans, 110, C06007, doi:06010.01029/02004JC002715, 2005.

Jiang, M. S. and Chai, F.: Physical control on the seasonal cycle of surface pCO_2 in the equatorial Pacific, Geophys. Res. Lett., 33, L23608, doi:10.1029/2006GL027195, 2006.

Kalnay, E., Kanamitsu, M., Kistler, R., Collins, W., Deaven, D., Gandin, L., Iredell, M., Saha, S., White, G., Woollen, J., Zhu, Y., Chelliah, M., Ebisuzaki, W., Higgins, W., Janowiak, J., Mo, K. C., Ropelewski, C., Wang, J., Leetmaa, A., Reynolds, R., Jenne, R., and Joseph, D.: The NCEP/NCAR 40-year reanalysis project, B. Am. Meteorol. Soc., 77, 437–471, 1996.

Le Borgne, R., Barber, R. T., Delcroix, T., Inoue, H. Y., Mackey, D. J., and Rodier, M.: Pacific warm pool and divergence: temporal and zonal variations on the equator and their effects on the biological pump, Deep-Sea Res. Pt. II, 49, 2471–2512, 2002.

Le Quéré, C., Orr, J. C., Monfray, P., Aumont, O., and Madec, G.: Interannual variability of the oceanic sink of CO_2 from 1979 through 1997, Global Biogeochem. Cy., 14, 1247–1265, 2000.

Lee, K., Wanninkhof, R., Takahashi, T., Doney, S. C., and Feely, R. A.: Low interannual variability in recent oceanic uptake of atmospheric carbon dioxide, Nature, 396, 155–159, 1998.

Liss, P. S. and Merlivat, L.: Air-sea gas exchange rates: introduction and synthesis, in: The Role of Air-Sea Exchange in Geochemical Cycling, edited by: Buatmenard, P. D., Reidel, Hingham, Mass., 113–129, 1986.

McGillis, W. R., Edson, J. B., Ware, J. D., Dacey, J. W. H., Hare, J. E., Fairall, C. W., and Wanninkhof, R.: Carbon dioxide flux techniques performed during GasEx-98, Mar. Chem., 75, 267–280, 2001.

McGillis, W. R., Edson, J. B., Zappa, C. J., Ware, J. D., McKenna, S. P., Terray, E. A., Hare, J. E., Fairall, C. W., Drennan, W., Donelan, M., DeGrandpre, M. D., Wanninkhof, R., and Feely, R. A.: Air-sea CO_2 exchange in the equatorial Pacific, J. Geophys. Res.-Oceans, 109, C08S02, doi:10.1029/2003JC002256, 2004.

BGD
7, 3879–3910, 2010

McKinley, G. A., Follows, M. J., and Marshall, J.: Mechanisms of air-sea CO_2 flux variability in the equatorial Pacific and the North Atlantic, Global Biogeochem. Cy., 18, GB2011, doi:10.1029/2003GB002179, 2004.

McPhaden, M. J.: Tropical Pacific Ocean heat content variations and ENSO persistence barriers, Geophys. Res. Lett., 30, 1480, doi:10.1029/2003GL016872, 2003.

McPhaden, M. J., Zebiak, S. E., and Glantz, M. H.: ENSO as an integrating concept in Earth science, Science, 314, 1740–1745, doi:10.1126/science.1132588, 2006.

Murtugudde, R., Seager, R., and Busalacchi, A.: Simulation of the tropical oceans with an ocean GCM coupled to an atmospheric mixed-layer model, J. Climate, 9, 1795–1815, 1996.

Naegler, T.: Reconciliation of excess C-14-constrained global CO_2 piston velocity estimates, Tellus B, 61, 372–384, doi:10.1111/j.1600-0889.2008.00408.x, 2009.

Nightingale, P. D., Malin, G., Law, C. S., Watson, A. J., Liss, P. S., Liddicoat, M. I., Boutin, J., and Upstill-Goddard, R. C.: In situ evaluation of air-sea gas exchange parameterizations using novel conservative and volatile tracers, Global Biogeochem. Cy., 14, 373–387, 2000.

Obata, A. and Kitamura, Y.: Interannual variability of the sea-air exchange of CO_2 from 1961 to 1998 simulated with a global ocean circulation-biogeochemistry model, J. Geophys. Res., 108, 3337, doi:10.1029/2001JC001088, 2003.

Olsen, A., Wanninkhof, R., Trinanes, J. A., and Johannessen, T.: The effect of wind speed products and wind speed-gas exchange relationships on interannual variability of the air-sea CO_2 gas transfer velocity, Tellus B, 57, 95–106, 2005.

Patra, P. K., Maksyutov, S., Ishizawa, M., Nakazawa, T., Takahashi, T., and Ukita, J.: Interannual and decadal changes in the sea-air CO_2 flux from atmospheric CO_2 inverse modeling, Global Biogeochem. Cy., 19, GB4103, doi:10.1029/2004GB002257, 2005.

Picaut, J., Ioualalen, M., Delcroix, T., Masia, F., Murtugudde, R., and Vialard, J.: The oceanic zone of convergence on the eastern edge of the Pacific warm pool: a synthesis of results and implications for El Niño-Southern Oscillation and biogeochemical phenomena, J. Geophys. Res., 106, 2363–2386, 2001.

Popova, E. E. and Anderson, T. R.: Impact of including dissolved organic matter in a global ocean box model on simulated distributions and fluxes of carbon and nitrogen, Geophys. Res. Lett., 29, 1303, doi:10.1029/2001GL014274, 2002.

Rixen, T., Guptha, M. V. S., and Ittekkot, V.: Deep ocean fluxes and their link to surface ocean processes and the biological pump, Prog. Oceanogr., 65, 240–259, 2005.

BGD

7, 3879–3910, 2010

Spatial and temporal variations in the sea surface in the equatorial Pacific

X. J. Wang

Sabine, C. L., Wanninkhof, R., Key, R. M., Goyet, C., and Millero, F. J.: Seasonal CO_2 fluxes in the Tropical and Subtropical Indian Ocean, Mar. Chem., 72, 33–53, 2000.

Takahashi, T., Feely, R. A., Weiss, R. F., Wanninkhof, R. H., Chipman, D. W., Sutherland, S. C., and Takahashi, T. T.: Global air-sea flux of CO_2 – an estimate based on measurements of sea-air pCO_2 difference, P. Natl. Acad. Sci. USA, 94, 8292–8299, 1997.

Takahashi, T., Sutherland, S. C., Sweeney, C., Poisson, A., Metzl, N., Tilbrook, B., Bates, N., Wanninkhof, R., Feely, R. A., and Sabine, C.: Global sea-air CO_2 flux based on climatological surface ocean pCO_2, and seasonal biological and temperature effects, Deep-Sea Res. Pt. II, 49, 1601–1622, 2002.

Takahashi, T., Sutherland, S. C., Feely, R. A., and Cosca, C. E.: Decadal variation of the surface water pCO_2 in the Western and Central equatorial Pacific, Science, 302, 852–856, 2003.

Takahashi, T., Sutherland, S. C., Wanninkhof, R., Sweeney, C., Feely, R. A., Chipman, D. W., Hales, B., Friederich, G., Chavez, F., Sabine, C., Watson, A., Bakker, D. C. E., Schuster, U., Metzl, N., Yoshikawa-Inoue, H., Ishii, M., Midorikawa, T., Nojiri, Y., Körtzinger, A., Steinhoff, T., Hoppema, M., Olafsson, J., Arnarson, T. S., Tilbrook, B., Johannessen, T., Olsen, A., Bellerby, R., Wong, C. S., Delille, B., Bates, N. R., and de Baar, H. J. W.: Climatological mean and decadal change in surface ocean pCO_2, and net sea-air CO_2 flux over the global oceans, Deep-Sea Res. Pt. II, 56, 554–577, 2009.

Wang, X. J., Christian, J. R., Murtugudde, R., and Busalacchi, A. J.: Ecosystem dynamics and export production in the Central and Eastern equatorial Pacific: a modeling study of impact of ENSO, Geophys. Res. Lett., 32, L02608, doi:02610.01029/02004GL021538, 2005.

Wang, X. J., Christian, J. R., Murtugudde, R., and Busalacchi, A. J.: Spatial and temporal variability in new production in the equatorial Pacific during 1980–2003: physical and biogeochemical controls, Deep-Sea Res. Pt. II, 53, 677–697, 2006a.

Wang, X. J., Christian, J. R., Murtugudde, R., and Busalacchi, A. J.: Spatial and temporal variability of the surface water pCO_2 and air-sea CO_2 flux in the equatorial Pacific during 1980–2003: a basin-scale carbon cycle model, J. Geophys. Res., 111, C07S04, doi:10.1029/2005jc002972, 2006b.

Wang, X. J., Le Borgne, R., Murtugudde, R., Busalacchi, A. J., and Behrenfeld, M.: Spatial and temporal variations in dissolved and particulate organic nitrogen in the equatorial Pacific: biological and physical influences, Biogeosciences, 5, 1705-1721, doi:10.5194/bg-5-1705-2008, 2008.

BGD

7, 3879–3910, 2010

Spatial and temporal variations in the sea surface in the equatorial Pacific

X. J. Wang

Wanninkhof, R.: Relationship between wind speed and gas exchange over the ocean, J. Geophys. Res., 97, 7373–7382, 1992.
Wanninkhof, R., Doney, S. C., Peng, T.-H., Bullister, J. L., Lee, K., and Freely, R. A.: Comparison of methods to determine the anthropogenic CO_2 invasion into the Atlantic Ocean, Tellus B, 51, 551–530, 1999.
Wanninkhof, R. and McGillis, W. R.: A cubic relationship between air-sea CO_2 exchange and wind speed, Geophys. Res. Lett., 26, 1889–1892, 1999.
Wanninkhof, R., Sullivan, K. F., and Top, Z.: Air-sea gas transfer in the Southern Ocean, J. Geophys. Res.-Oceans, 109, C08S19, doi:10.1029/2003JC001767, 2004.
Watson, A. J., Upstillgoddard, R. C., and Liss, P. S.: Air sea gas-exchange in rough and stormy seas measured by a dual-tracer technique, Nature, 349, 145–147, 1991.
Weiss, R. F. and Price, B. A.: Nitrous-oxide solubility in water and seawater, Mar. Chem., 8, 347–359, 1980.

BGD
7, 3879–3910, 2010

Table 1. Values of biogeochemical parameters used in the non-DON model (Wang et al., 2006a) and the DON model (Wang et al., 2008).

Parameter	Symbol	Unit	non-DON	DON
Maximum growth rate at 0 °C	μ_{L0}	d^{-1}	0.58	1.16
Half saturation constant for iron limitation	K_{S_Fe}	$nmol\,m^{-3}$	30	14
	K_{L_Fe}	$nmol\,m^{-3}$	110	150
Phytoplankton mortality rate	m_S	d^{-1}	0.2	0.17
	m_L	d^{-1}	0.15	0.31
Maximum grazing rate	g_{PS}	d^{-1}	2.8	2.9
	g_{PL1}	d^{-1}	1.5	1.2
	g_{ZS}	d^{-1}	1.4	1.7
Zooplankton excretion rate	r_S	d^{-1}	0.1	0.28
	r_L	d^{-1}	0.08	0.22
Zooplankton mortality rate	δ_S	d^{-1}	0.15	0.12
	δ_L	d^{-1}	0.1	0.09
Decomposition rate	c_{S0}	d^{-1}	0.03	0.01
	c_{L0}	d^{-1}	0.03	0.0055
	c_{DON}	d^{-1}	N/A	0.0008–0.0025

BGD
7, 3879–3910, 2010

Table 2. Primary productivity (mmol C m^{-2} d^{-1}) estimated from the models and field measurements.

Year	Month	Latitude	Longitude	non-DON	DON	Data	Reference
1992	Feb	5° N–5° S	140° W	26–43	37–67	50–80	A
1992	Mar	5° N–5° S	125° W–110° W	56–63	43–90	52–63	B
1992	Apr	5° N–5° S	170° W–140° W	36–56	21–62	53–76	B
1992	Sep	5° N–5° S	140° W–125° W	64–81	45–92	73–78	B
1992	Nov	5° N–5° S	110° W–95° W	47–50	36–80	70–75	B
1994	Oct	0°	150° W	95	101	90–104	C
1996	Apr	2° N–2° S	165° E–175° E	45–65	41–84	56–99	C
1996	May	0°	150° W–170° W	70–93	83–112	76–95	C
1996	Oct	5° N–5° S	180°	40–85	21–91	50–70	D

A: Barber et al. (1996)
B: Chavez et al. (1996)
C: Aufdenkampe et al. (2002)
D: Le Bouteiller et al. (2003)

BGD
7, 3879–3910, 2010

Table 3. Mean and standard deviation (SD) of averaged ΔpCO_2 (µatm) and integrated outgassing (Pg C yr^{-1}) over the area of 150° E–90° W, 10° N–10° S during 1990–2007.

Experiment	ΔpCO_2		Outgassing	
	Mean	SD	Mean	SD
W-92	52.2	10.2	0.42	0.12
W-99	72.7	12.2	0.32	0.10
M-01	55.4	10.7	0.39	0.10
M-04	44.0	9.8	0.44	0.10

BGD
7, 3879–3910, 2010

Table 4. Comparisons of mean and standard deviation (SD) of integrated rates (mmol C m^{-2} d^{-1}) of primary productivity (PP), net community production (NCP), and carbon regeneration (CR) over 0–50 m, averaged ΔpCO_2 (µatm) and net sea-to-air CO_2 flux (Pg C yr^{-1}) between the non-DON model and DON model for the period of 1990–2003.

	Non-DON model			DON model			Difference	
Parameters	Mean	SD	Var* (%)	Mean	SD	Var* (%)	Absolute	Relative (%)
			Wyrtki Box (180°–90° W, 5° N–5° S)					
PP	47.4	9.9	21	40.9	7.2	18	6.5	14.7
NCP	11.9	4.5	38	12.6	3.4	27	−0.7	−5.7
CR	35.5	6.5	18	28.3	4.5	16	7.2	22.5
ΔpCO_2	93.5	10.8	12	79.5	18.2	23	14.0	16.2
CO_2 flux	0.25	0.06	24	0.21	0.07	33	0.04	17.4
			Basin (140° E–90° W, 14° N–14° S)					
PP	25.1	4.3	17	20.2	3.1	15	4.9	21.6
NCP	5.2	1.7	33	5.7	1.2	21	−0.5	−9.2
CR	19.9	3.0	15	14.5	2.3	15	5.4	31.4
ΔpCO_2	57.8	5.3	9	37.6	7.5	20	20.2	42.3
CO_2 flux	0.67	0.11	16	0.41	0.13	32	0.26	48.1

* $\text{Var} = \frac{\text{SD}}{\text{Mean}}$

BGD
7, 3879–3910, 2010

Table 5. Mean, maximum, minimum and standard deviation (SD) of averaged ΔpCO_2 (µatm) and integrated outgassing (Pg C yr^{-1}) over 140° E–90° W, 14° N–14° S.

Experiment	ΔpCO_2		Outgassing	
	1995	2000	1995	2000
Mean	43.5	46.9	0.49	0.54
Maximum	50.8	53.3	0.68	0.62
Minimum	33.8	42.6	0.31	0.37
SD	4.9	3.4	0.13	0.08

BGD
7, 3879–3910, 2010

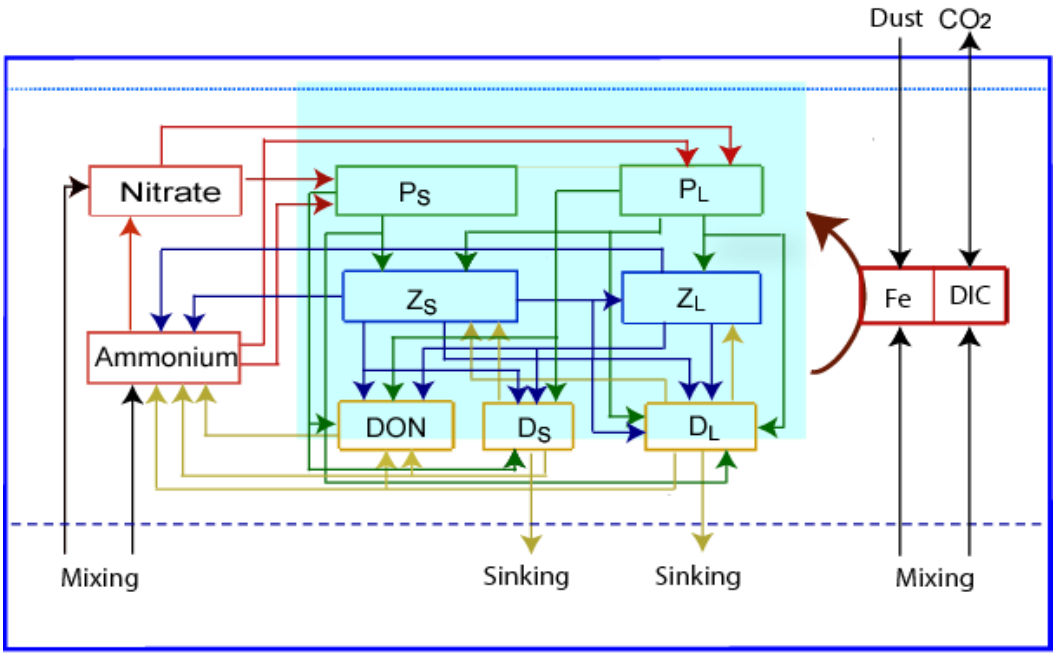

Fig. 1. Diagram of the dynamic marine ecosystem-carbon model. Red, green, blue and yellow lines and arrows denote nitrogen fluxes originating from inorganic forms, phytoplankton cells, zooplankton cells, and DOM and detritus, respectively. Black lines and arrows denote physical supply of nutrients.

BGD
7, 3879–3910, 2010

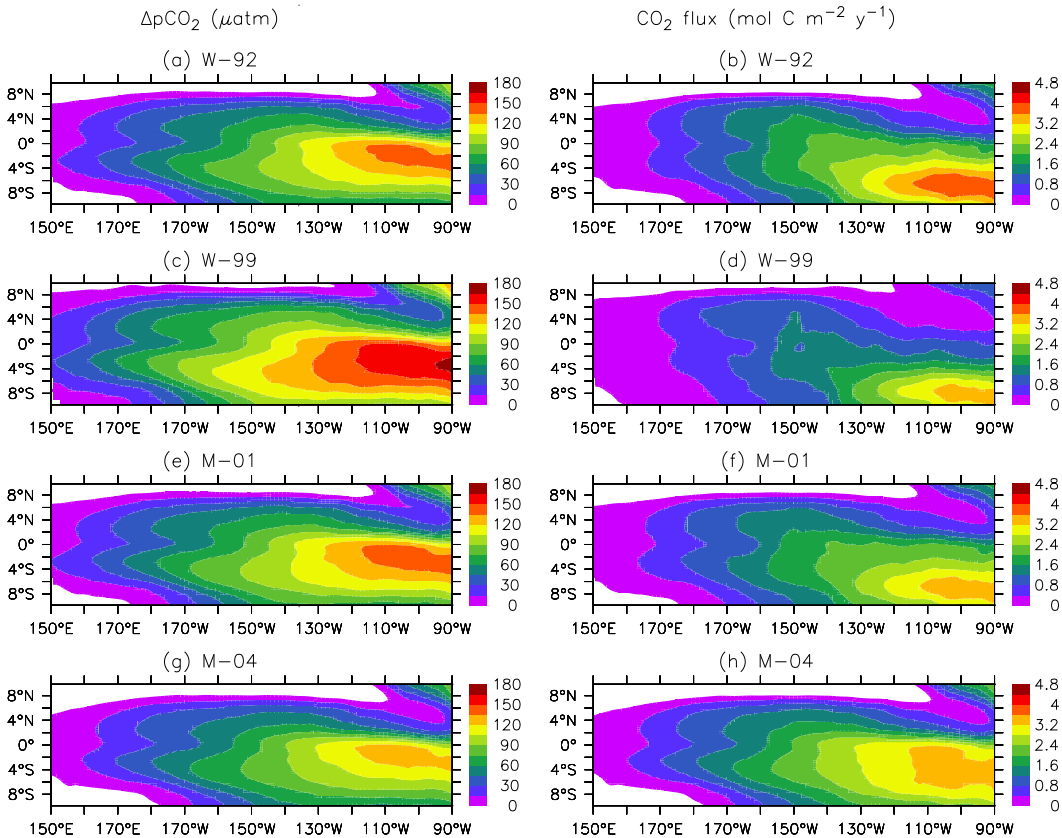

Fig. 2. Modeled climatology (1990–2007) of sea minus air pCO_2 (ΔpCO_2) (left column) and sea to air CO_2 flux (right column) from **(a)** and **(b)** W-92, **(c)** and **(d)** W-99, **(e)** and **(f)** M-01, and **(g)** and **(h)** M-04 simulations.

BGD
7, 3879–3910, 2010

Spatial and temporal variations in the sea surface in the equatorial Pacific

X. J. Wang

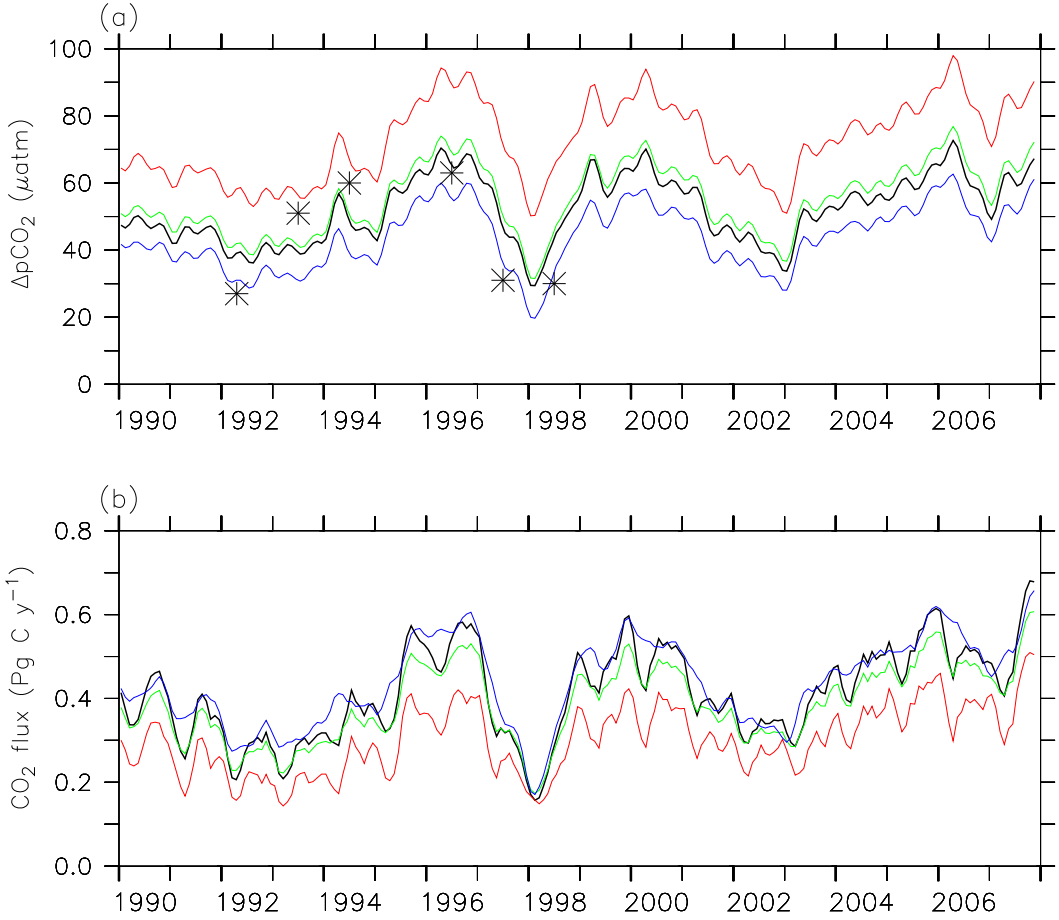

Fig. 3. Interannual variations of **(a)** averaged ΔpCO_2 and **(b)** integrated rates of sea to air CO_2 fluxes from W-92 (black), W-99 (red), M-01 (green) and M-04 (blue) simulations in the entire basin (150° E–90° W, 10° N–10° S).

BGD
7, 3879–3910, 2010

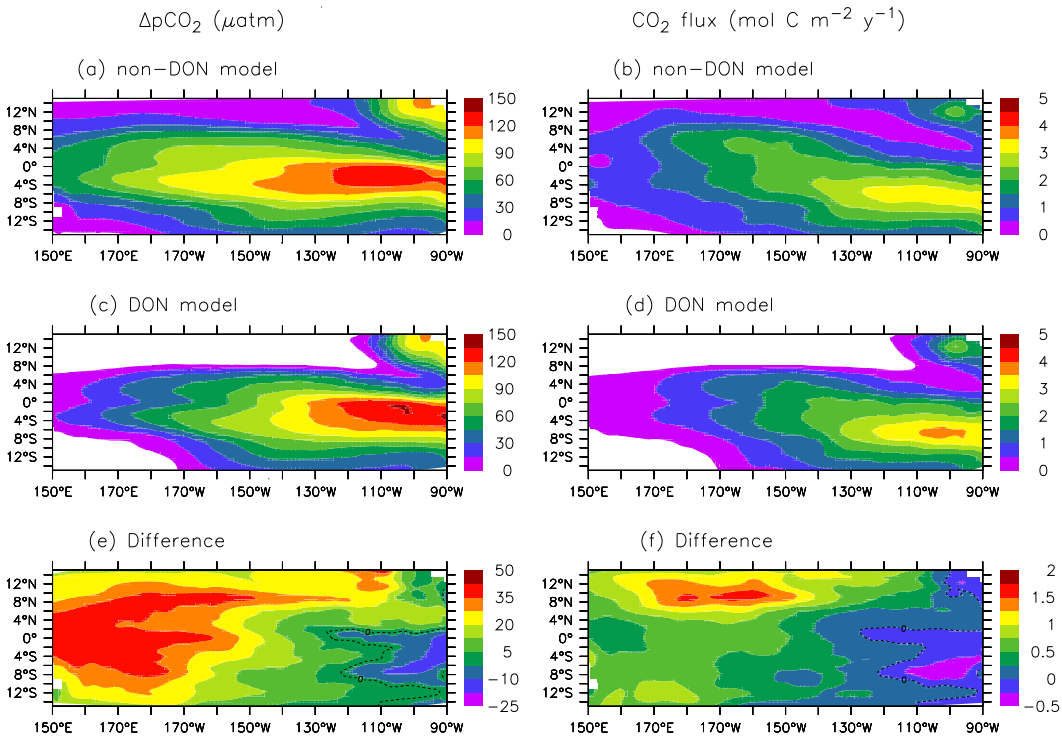

Fig. 4. Simulated climatology (1990–2003) of sea minus air pCO_2 (ΔpCO_2) (left column) and sea to air CO_2 flux (right column) from **(a)** and **(b)** the non-DON model, **(c)** and **(d)** the DON model, and **(e)** and **(f)** the difference (non-DON model minus DON model).

BGD
7, 3879–3910, 2010

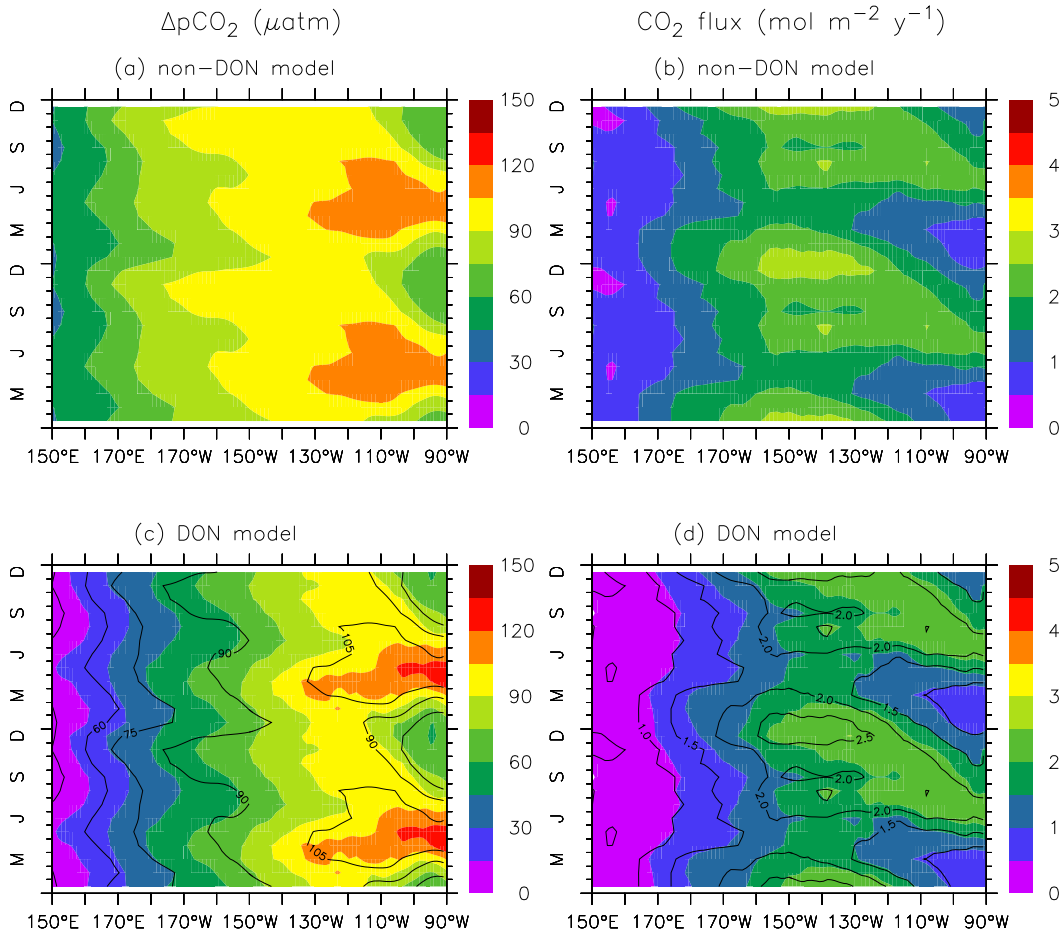

Fig. 5. Modeled seasonal climatology (with a repetition of another year) of sea minus air pCO_2 (left column) and sea to air CO_2 flux (right column) over 5° N–5° S from **(a)** and **(b)** the non-DON model, and **(c)** and **(d)** the DON model (color contour) vs. the non-DON model (black lines).

BGD
7, 3879–3910, 2010

Spatial and temporal variations in the sea surface in the equatorial Pacific

X. J. Wang

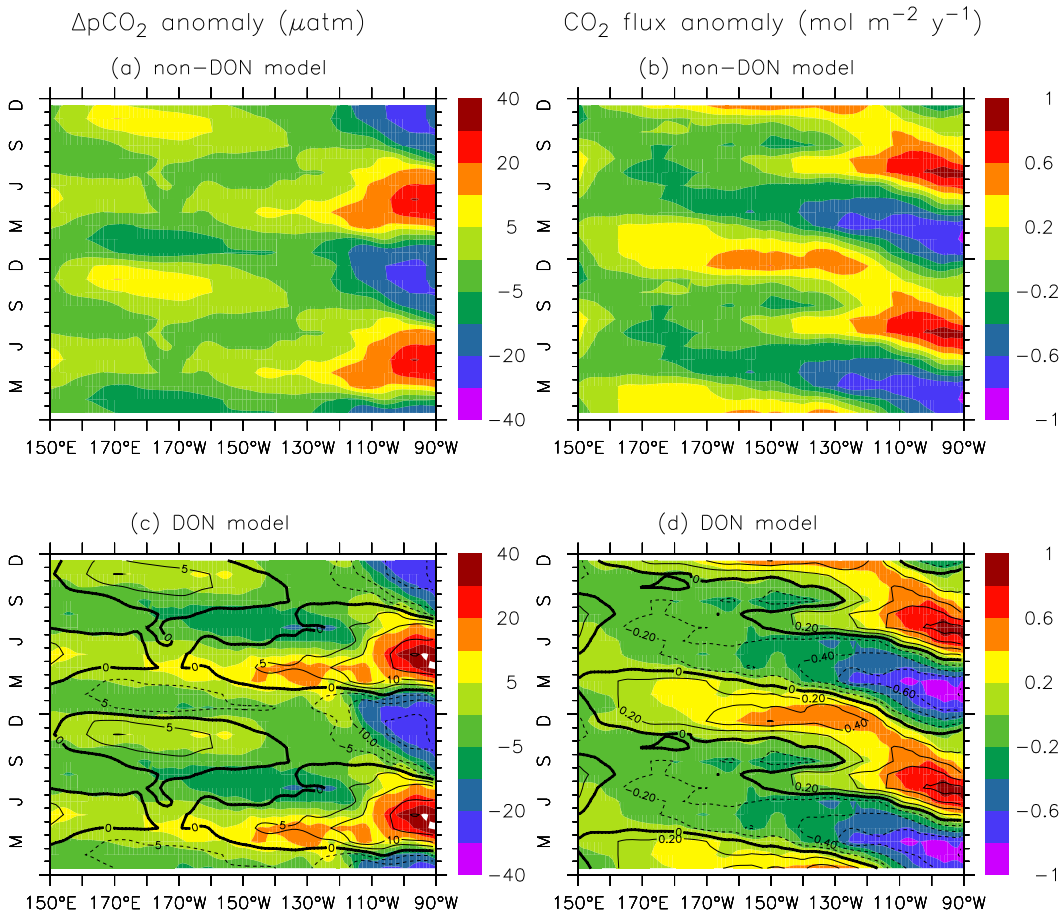

Fig. 6. Modeled seasonal climatology (with a repetition of another year) of anomalies for sea minus air pCO_2 (left column) and sea to air CO_2 flux (right column) over 5° N–5° S from **(a)** and **(b)** the non-DON model, and **(c)** and **(d)** the DON model (color contour) vs. the non-DON model (black lines).

BGD
7, 3879–3910, 2010

Spatial and temporal variations in the sea surface in the equatorial Pacific

X. J. Wang

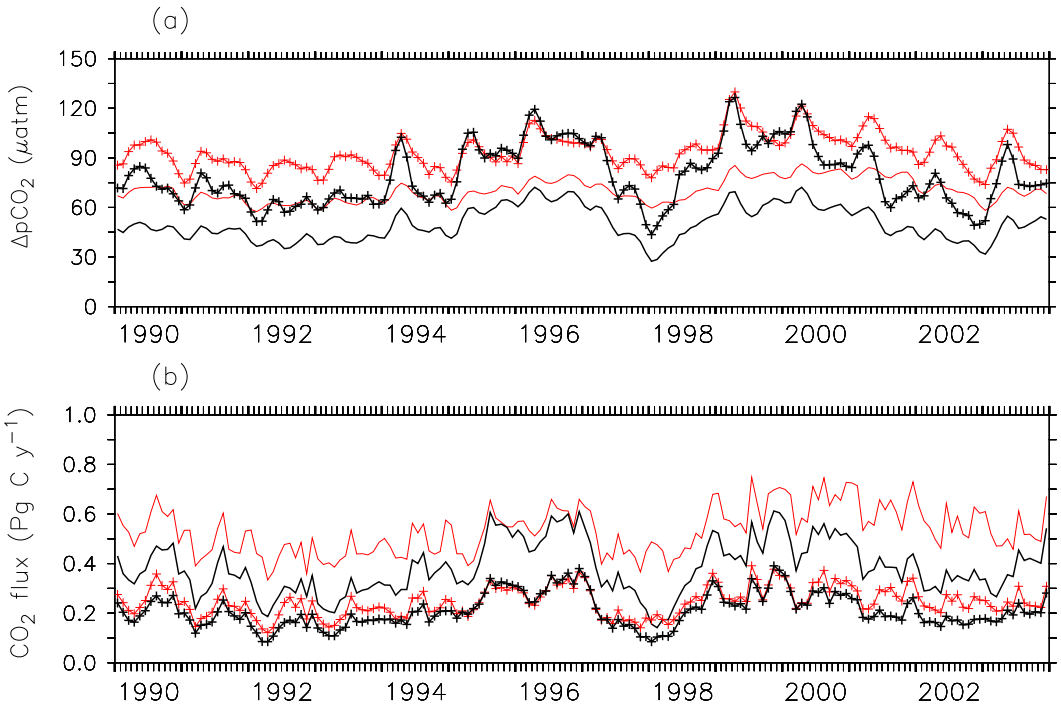

Fig. 7. Comparisons of **(a)** averaged sea minus air pCO_2, and **(b)** integrated sea to air CO_2 flux over the entire basin (150° E–90° W, 10° N–10° S) (lines) and in the Wyrtki box (180°–90° W, 5° N–5° S) (lines with crosses) from the non-DON model (red) and the DON model (black).

BGD
7, 3879–3910, 2010

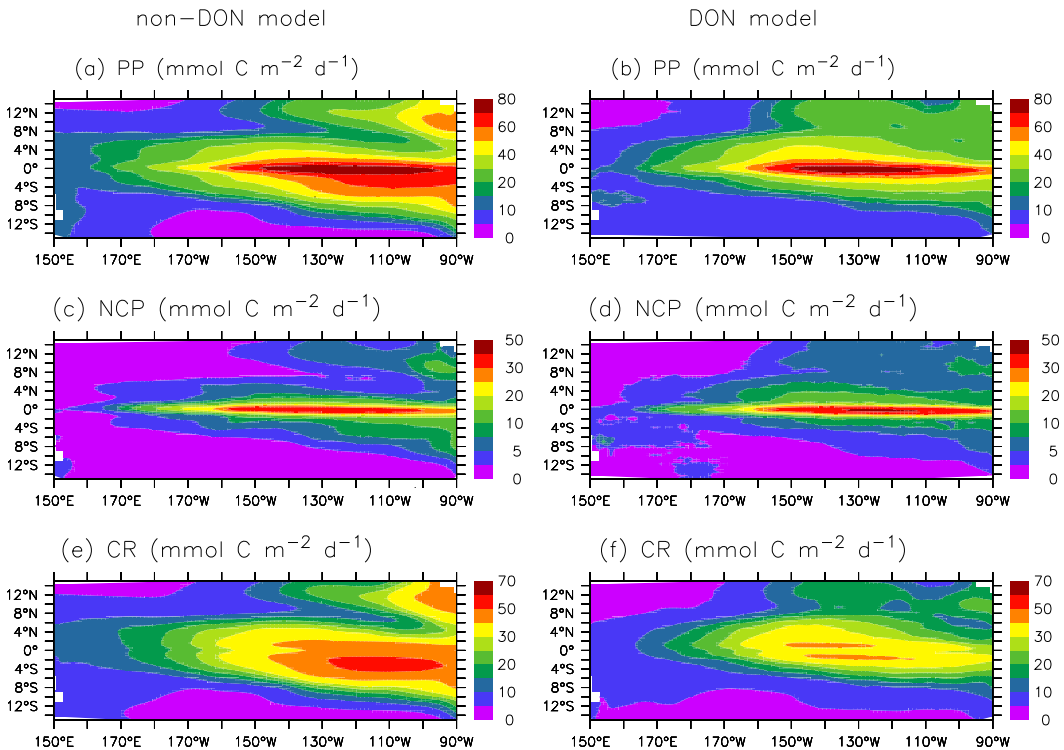

Fig. 8. Simulated climatology (1990–2003) of **(a)** and **(b)** primary productivity (PP), **(c)** and **(d)** net community production (NCP), and **(e)** and **(f)** carbon regeneration (CR) integrated over the upper 50 m from the non-DON model (left column) and the DON model (right column).

BGD
7, 3879–3910, 2010